Detection of Tool Flute Breakage in End Milling Using Feed-Motor Current Signatures

Xiaoli Li

***Abstract*—In this paper, an effective algorithm based on improved time-domain averaging is proposed to detect tool flute breakage during end milling using feed-motor current signatures. The algorithm proposed is demonstrated to be effective in detecting tool flute breakage in real time through a series of milling experiments, and is also demonstrated to be insensitive to the effects for transients, such as cutter runout, entry/exit cuts, and noise in the feed-motor current signals. Results indicated that the approach showed excellent potential for practical, on-line application for tool flute breakage detection during end milling.**

***Index Terms*—End milling, flute breakage, time-domain averaging.**

I. Introduction

THE END milling is a multipoint cutting operation that is well suited for the machining of thin-wall sections, slotting, as well as contouring, so as to be widely employed in automobile, aircraft, and military industries. The successful application of tool breakage detection to end milling not only ensures high quality parts, but also safeguards the machining system. For the end milling, the tool breakage is divided into primarily two types: shank breakage and flute breakage. The shank breakage is one of the most severe forms for tool failure, which is readily evident from the cutting force, motor current, and acoustic emission (AE) signatures. The flute breakage, on the other hand, may be subtle in nature so as to be undetected for a period of time. Note that the undetected flute breakage not only increases the potential for further tool damage, but also affects the surface finish of the machined parts. Real time response to flute breakage during end milling may prevent the workpiece and machining system from becoming excessively damaged. Research to date has presented four main approaches to detect tool flute breakage for the end milling [15], shown in Fig. 1. Cutting force and AE-based techniques [21], however, are two primary methods.

Significant research has been done on cutting force-based tool flute breakage detection [1]–[4], [16]. The technique is dependent upon the instantaneous load applied to the cutter and has the advantage of being easily modeled. Cutting force measurements are commonly taken using a dynamometer mounted on a machining worktable, or a mounted tool holder during machining. The dynamometer is an essential tool for experimental work, and has been proved a very successful tool in establishing inter-

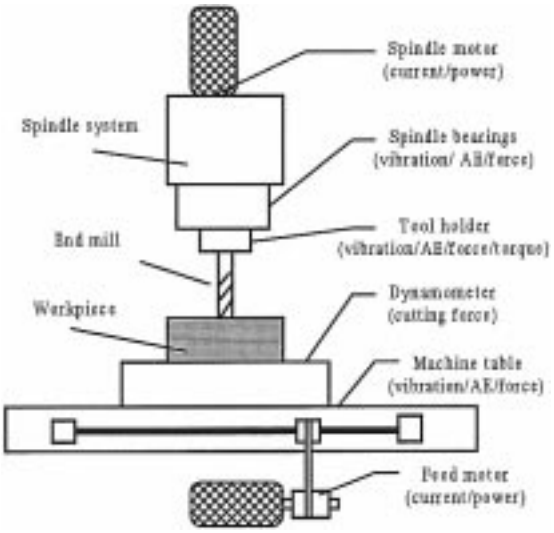

Fig. 1. Approaches of tool breakage monitoring for end milling operations.

relationships between secondary machining parameters and cutting force, so as to enable researchers to prove their tool monitoring strategies prior to implementing them on-line. However, the physical characteristics of the dynamometer mounted on the worktable seriously limit the physical size of the workpiece, on the other hand, mounted in on the tool holder interrupts the change of cutting tools, and the cost of the dynamometer is very high. Additionally, the cutting force-based methods often require complex signal processing techniques, like high-order time series models, and FFT, as well as time-frequency analysis, which result in a hindrance to real time application due to the computation time.

Acoustic emission (AE), is a very high frequency stress wave, generated when deformation occurs when metals are cut or fractured, which is linked to the plastic deformation process occurring during chip formation due to the interaction between the workpiece and cutting tool. Experimental results showed that large AE bursts are generated at the instance of tool breakage. Based on the phenomena, AE signal has been very successful in its application to tool breakage monitoring in signal-point cutting, like turning operations [5]–[8]. Its application to the end milling, however, has been less straightforward. One is that, the end milling process is interrupted cutting operations, pulse shock loading occurs during the entry and exit of each individual tooth to the workpiece. It is possible that the magnitude of these shock pulses is equivalent to those generated during tooth fractures, such as tool flute breakage. On the other hand, how to locate AE sensor to obtain AE signals from the rotating cutting tools is a difficult question. Although, Hutton [9] de-

Manuscript received June 10, 2000; revised Oct. 13, 2000. Recommended by Technical Editor R. Isermann.

The author is with the Institute for Production Engineering and Machine Tools, University of Hannover, D-30159, Hannover, Germany, on leave from the School of Electric Engineering, Yanshan University, Qinhuangdao, 066004, China (e-mail: lixiaoli_hit@yahoo.com).

Publisher Item Identifier S 1083-4435(01)10736-2.

veloped a liquid-coupled sensor system, mounted on the end of spindle, for collecting AE signals derived from cutter through tool holder; Li and Yuan [10] also developed a simple device for collecting AE signals from tool holder through magnetofliud. The fixed simple devices all alter the structure of machine tools more or less, and how to let these devices work effectively also is not very easy during its application processing. Furthermore, AE signals are highly dependent upon cutting conditions and tool and workpiece material/geometry, so as to require trial cuts in order to determine a proper threshold value. Accordingly, AE-based flute breakage monitoring leads to missed breakage events and excessive false alarms during end milling.

Spindle or feed-motor current-based tool breakage monitoring systems have been presented in the end milling operations for overcoming the disadvantages of cutting force and AE based methods [18], [22]. In [11], authors developed a time series autoregressive model to analyze spindle motor current and the difference between the actual current and that predicted by the model, the residual, was then used as an indication of tool breakage during the end milling. In [12], Altintas proposed a tool breakage monitoring strategy using the indirect cutting force estimated by dc motor current measurement. A similar method is developed in [13] to monitor the ac motor currents of feed drive system, a first order autoregressive model of the motor current provides an indication of tool breakage using an analysis of the difference between the predicted and actual motor current. Whilst, the paper also presented a second monitoring index and cutter insert self-comparing to make the system less sensitive to cutter runout.

This paper applies improved time-domain averaging to construct a new algorithm to detect flute breakage during the end milling through the feed-motor current signals. The proposed detection system demonstrated by the experiments can meet the following general requirements: reliable detection of tool failures; real time application; independent upon the cutting conditions and tool/workpiece material; insensitive to the changes of cutting conditions; and, low incidence of false alarms. These experiments included the entry/exit cuts, flute breakage during steady-state cutting, flute breakage on entry/exit cut, and the effects of cutting parameters.

II. Time-Domain Averaging

For repetitive signals resulting from rotating machines or some alternating mechanism, two processing methods have been extensively used: spectral analysis and time-domain averaging (TDA). The first one is usually intended to detect periodicities related to the main period, i.e., to obtain the harmonic components of the repetitive signals. The second one filters out a periodic signal time-locked to such a period, i.e., to obtain the period components of the repetitive signal.

Braun and Seth first presented TDA to process the signals with repetitive component [14]. The method can decompose the signals into repetitive and residual components, and the repetitive signals are again decomposed into truly periodic and random components. The decomposition of a signal, $X(t)$, is described by the following:

$$X(t) = X_p(t) + X_n(t) + n(t) \tag{1}$$

where $Xp(t)$ is the period term, i.e., $X_p(t) = X_p(t+T)$; $Xn(t)$ is the random repetitive term; $n(t)$ is the residual term not time-locked to a basic period T.

TDA, which is based on the averaging of points one period apart, is widely used to extract the signal $X_p(t)$ from the compound signal $X(t)$. TDA is computed as

$$X_P(j) = \frac{1}{P}\sum_{k=0}^{P-1} X(j+kM), \qquad j = 1, 2, \ldots, M \tag{2}$$

where $XP(j)$ denotes the average over P periods of the jth sample in the period, M is the number of samples per period and X is the analyzed signal.

A general description of the random, $Xn(t)$, could be based on the following expression

$$X_n(t) = g(t)X_r(t) \tag{3}$$

where $Xr(t)$ denotes a continuous random process of no obvious time pattern, and $g(t)$ is a deterministic period function of period T, i.e., $gr(t) = gr(t+T)$.

Based on above analysis, they presented a formal approach for analyzing repetitive signal. Denoting the signal as $X(j)$, one may define the two dimensional matrix

$$S(j, k) = X[j + kM], \qquad \begin{cases} j = 1, 2, \ldots, M \\ k = 0, 2, \ldots, P. \end{cases} \tag{4}$$

The averages of the dimensional vector of $S(j, k)$ are defined as the periodic component, $X_P(j)$, i.e.,

$$X_P(j) = \frac{1}{P}\sum_{k=0}^{P-1} S(j, k). \tag{5}$$

The time domain average is extended to the entire data sets is

$$X_P(i) = X_P(i - M), \qquad i = M + 1, \ldots, PM \tag{6}$$

and the residual at each point in the data set is calculated as

$$X_R(j) = X(j) - X_P(j), \qquad i = 1, 2, \ldots, PM. \tag{7}$$

III. Flute Breakage Detection Algorithm

The end milling processing exhibits a period generation mechanism, perturbed by the spindle speed variations, the tool conditions, and the effects of chips [17]. The ideal feed-motor current signal during end milling varies periodically with frequency, which is equal to the product of spindle rotational frequency and the number of cutting edges (flutes). A schematic illustrating the end milling processing is provided in Fig. 2 [4]. In order to present an effective algorithm for detecting tool flute breakage, we first have to analyze the changes of feed-motor current signal with the different cutting conditions.

A. Analysis of the Feed-Motor Current Signals

Fig. 3(a) displays a feed-motor current signal without cutting load at the feed speed of 120 mm/min. The motor current consumed mainly overcomes the viscous damping of feed system and friction of mechanical system. The feed-motor current signals are wave because of the different of the friction coefficients

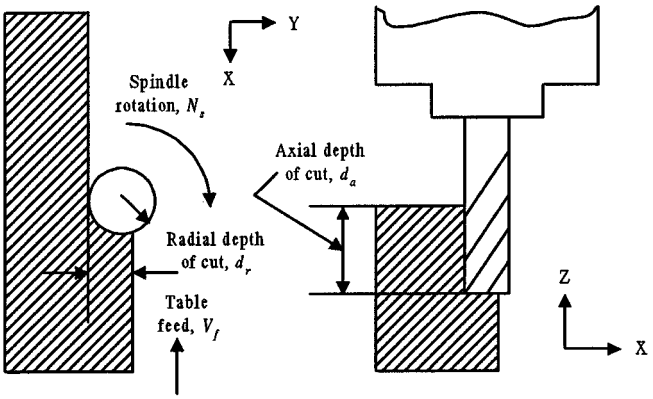

Fig. 2. Illustration of end milling process.

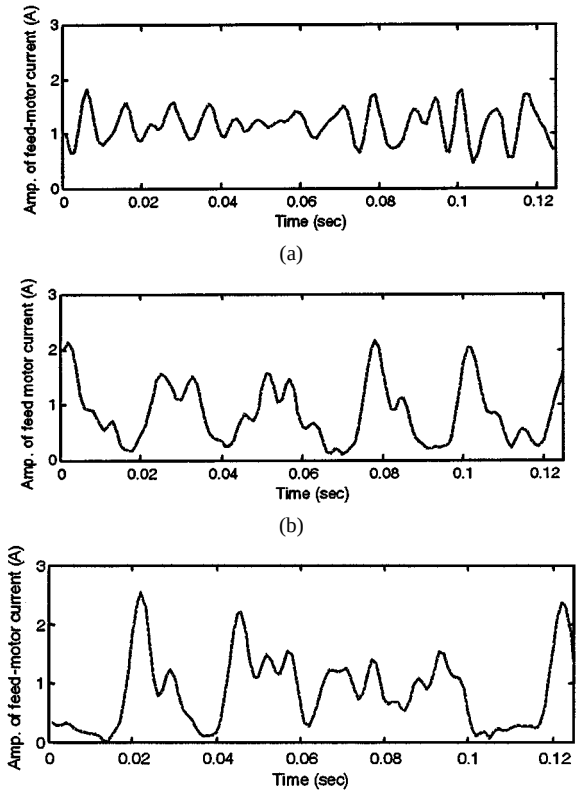

Fig. 3. Feed-motor current signals in end milling with different cutting conditions. Tool/workpiece material: HSS/45# steel; spindle speed: 600 rpm; radial depth of cut: 2 mm; axial depth of cut: 4 mm; feed speed: 120 mm/min; cutter diameter: 8 mm; cutter flute: 4. (a) Without cutting load. (b) Normal cutting condition. (c) One flute breakage condition.

on different position. When the end mill is normal condition, without flute breakage, the variation of motor current is similar to a regular periodic signal; this is shown in Fig. 3(b) that, to the eye, shows about 5 cycles during a sampling time of 0.001s resulting in a computed period of 0.025 s. This is equal to the theoretical period of 0.025 s corresponding to a four-flute cutter rotating at 600 rpm. Under the steady-state cutting, the pattern of feed-motor current signal is similar to that of feed cutting force, the conclusion has been verified in [13]. The regular periodic signals of motor current, however, is interrupted when the cutter occurs a flute breakage, this is shown in Fig. 3(c), and the figure of tool flute breakage is shown in Fig. 4. The dramatic

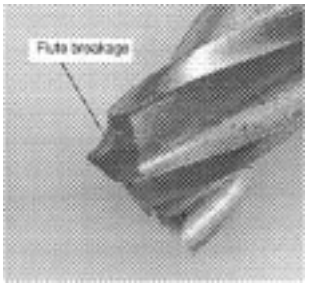

Fig. 4. Tool flute breakage for end milling (cutter diameter: 8 mm, cutter flute 4).

change in the feed-motor current signature occurs, in general, due to two phenomena. One is that following tool fracture; the broken flute encounters a reduced or negligible chip load, while the other flutes must absorb an increased chip load for compensating for the broken flute. The other phenomenon is that fracture tool material becomes "jammed" between the workpiece and subsequent flutes, thus greatly increases the cutting force [15], i.e., also increasing the feed-motor current. For both of these occurrences, the feed-motor current with flute breakage will be greater in oscillation than that without flute breakage.

B. Algorithm of TDA

In this paper, the time-domain averaging (TDA) method is used to decompose the compound repeated signal, feed-motor current in end milling $X(i)$, into a periodic component, $XP(i)$, and a residual component, $XR(i)$, i.e.

$$X(i) = X_P(i) + X_R(i), \qquad i = 1, 2, \ldots, N \tag{8}$$

where N is the length of the signals. For the feed-motor current generated during end milling under the bandwidth of the feed drive system, the frequency is equal to the reciprocal of the tooth passing frequency, such that: $f_P = N_f N_s/60$, where N_f is the number of cutting flutes, N_s is the cutter rotational speed in r/min (rpm). Given the sampling frequency f_s, the number of data points per period is: $M = f_s/f_P$. Thus the number of periods contained in a complete sample data is: $P = N/M$.

At corresponding times within each period, the periodic component X_P is computed as the average of the values obtained at that temporal position in every period contained in the sample data set is

$$X_p(j) = \frac{1}{P}\sum_{k=0}^{P-1} X(j + kM), \qquad j = 1, 2, \ldots, M. \tag{9}$$

The rest of period component $X_P(i)$ and $X_R(i)$ are calculated by (6) and (7). The residual at each ponit represents the variation of the observed feed-motor current signal relative to a uniform periodic signal.

C. Improved TDA Algorithm

In general, the M in (9) is not an integer, so that we use the rounding function to process that, i.e., $M = \mathrm{round}(f_s/f_P)$, results in that f_P is not equal to f_s/M, and $\Delta T = T_p - M/f_s$, as called the period cutting errors, where T_p is the period of the

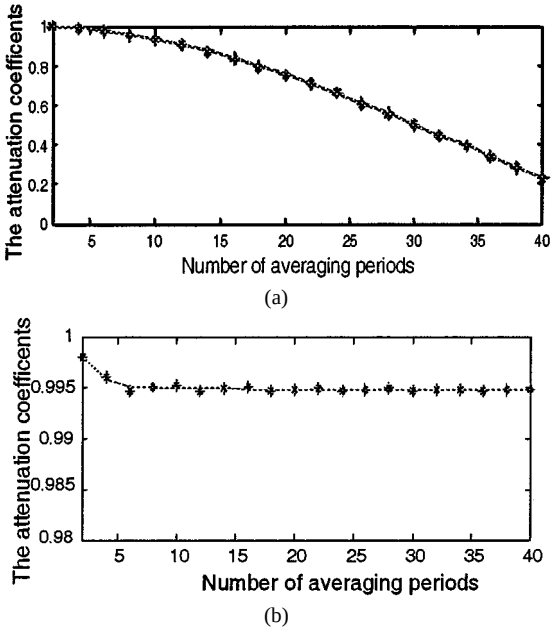

Fig. 5. The attenuation coefficients for different averaging period. (a) Original TDA. (b) Improved TDA.

interesting components. The influence of the period cutting errors should be analyzed before the use of the algorithm. Taking Z-transforms for (9), the corresponding transferring function, $H(f)$, is the following relation:

$$|H(f)| = \frac{1}{P}\left|\sin\left(\frac{\pi P f}{f_s}\,\text{round}\left(\frac{f_s}{f_P}\right)\right)\Big/ \sin\left(\frac{\pi f}{f_s}\,\text{round}\left(\frac{f_s}{f_P}\right)\right)\right|. \quad (10)$$

$|H(f_P)|$ is the attenuation coefficient of the interesting component at its basic frequency f_P. Fig. 5(a) shows that attenuation coefficients for different averaging period when we use the direct TDA to extract 60 Hz components from a time series with 1 kHz sampling frequency. In terms of the results above conclusion may be made: the more the periods of averaging, the larger the attenuation. Therefore, when taking a large value, P, the period cutting error has a bad influence on the effectiveness of TDA, the approach fail in separating the required component out.

To overcome the disadvantage of direct TDA mentioned, an improved algorithm is presented in [19], as shown in

$$X_p(j) = \frac{1}{P}\sum_{i=1}^{P-1} x(j+m_i), \qquad j = (P-1), \ldots, m_P \quad (11)$$

where $m_i = \text{round}(iM)$. Taking Z-transforms for (11), the corresponding transferring function shows as follows:

$$|H(f)| = \frac{1}{P}\left|\sum_{i=0}^{P-1}\exp\left(-j2\pi\,\frac{f}{f_s}\,\text{round}\left(\frac{if_s}{f_P}\right)\right)\right|. \quad (12)$$

Fig. 5(b) shows that the attenuation coefficients for different averaging period when we use the improved algorithm to extract 60 Hz components from a time series with 1000-Hz sampling frequency. In terms of the results above, we may make a different conclusion from the transitional TDA: with the increase in the number of averaging periods, the attenuation coefficients are basically kept unchanged. In the improved algorithm, the influence of the period cutting error on the decomposed results is basically controlled.

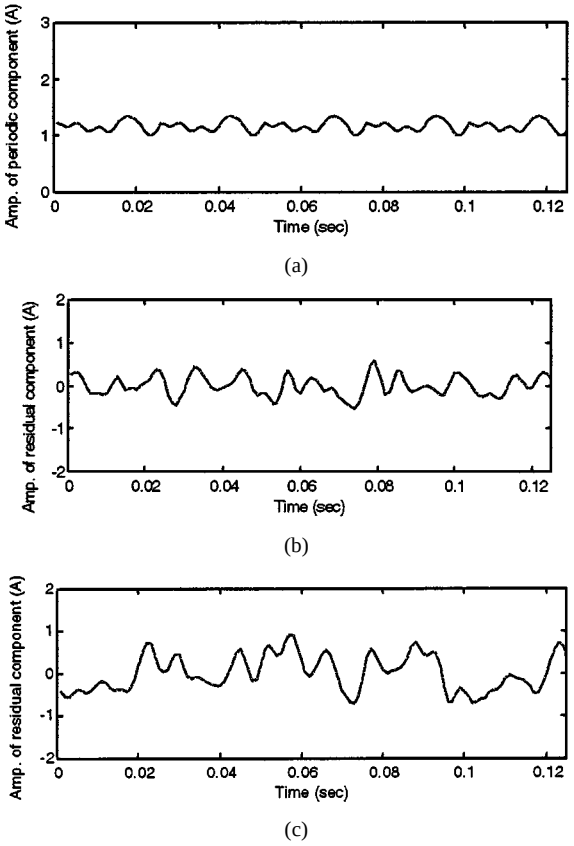

Fig. 6. The residual components of feed-motor current signals. (a) Without cutting load. (b) With cutting load. (c) With a tool flute breakage.

D. Monitoring Feature

Using the improved TDA algorithm TDA to decomposing the feed-motor current signals provided in Fig. 3, the results are shown in Fig. 6. Fig. 6(a) is the residual components of feed-motor current signals without cutting load; Fig. 6(b) is the residual components of feed-motor current signals under steady-state cutting; and Fig. 6(c) displays the residual components of feed-motor current signals with a flute breakage. It is found that the amplitude of residual component fluctuates severely when the cutter occurs flute breakage by comparing Fig. 6(a) and (b) with (c). In this paper, therefore, the mean of residual components, X_D, of the feed-motor current generated during end milling is used as a feature of tool flute breakage detection. It can be calculated by the following:

$$X_D = \frac{1}{M}\sum_{j=1}^{M}\left(\frac{1}{P}\sum_{k=0}^{P-1} X_R^2(j+kM)\right). \quad (13)$$

E. Detection of Tool Flute Breakage

To eliminate the effects of unexpected noise, a median filter is used to process the monitoring feature series before it is applied to detect the tool flute breakage during end milling. Then, the

rest of problem is how to set up a threshold to detect the tool flute breakage, based on the monitoring feature series $X_D(i)$, for the real time monitoring system. Considering the effects of changes of cutting conditions, a float threshold is designed to detect the flute breakage based on the monitoring feature series during end milling in this paper. The calculation of the float threshold is given by

$$FT(i) = \left(\frac{1}{M}\sum_{j=1}^{M} X_D(i-j+1)\right)\left(1+c^2\right) \qquad (14)$$

where M is the number of the selected monitoring feature series and c is the specified risk coefficient for determining "detection limit." In terms of the real time requirements of the flute breakage detection, the number of the selected monitoring feature series does not admitted to be a large value. In this paper it is selected to be three. The risk coefficient c is associated with the concluding that a flute breakage has occurred. A very large value for c produces wide detection limits, which makes the identification strategy less sensitive allowing actual flute breakages to go undetected. A very small value for c, on the other hand, produces narrow detection limits, which results in a large number of flute breakage false alarms. In practice, a value c should be selected based on the consequences of failing to detect flute breakage [20]. For the purpose of this paper, a value for c of 0.65 is selected.

IV. Experimental Procedure

All experiments were performed on a CNC Vertical Machining Centre (Mazak AJV 25/405) with the ac permanent magnet synchronous motors. The experimental set up is as shown in Fig. 7. Three current sensors (Hall Effect Current Transducer, Stock no. 286-327) are used to measure the 3-phases currents of feed-motor I_U, I_V, and I_W, and through a low-passed (50 Hz) filter, respectively. The root mean square (rms) of feed-motor current, $I_{\rm rms}$, can be calculated by (15),

$$I_{rms} = \sqrt{\tfrac{1}{3}\left(I_U^2 + I_V^2 + I_W^2\right)}. \qquad (15)$$

This method, which is very simple and widely used in the industry, uses the rms value for converting the ac current to the equivalent dc current.

A set of experiments was performed so as to test the reliability of flute detection algorithm under actual cutting conditions. These tests included entry/exit cuts, flute breakage during steady-state cutting, changed cutting parameters; and flute breakage on entry/exit cuts. All of the tests were performed under dry conditions in down milling mode, the sampling frequency was set as 1 kHz. Additionally, the maximum tooth frequency used in the tests should be less than 67 Hz, this is determined by the bandwidth of feed servo system. The tool/work piece material was selected as HSS/45# steel.

V. Experimental Results

A. Entry/Exit Cut

The insensitivity of the algorithm to entry/exit cut is demonstrated by following test. Fig. 8(a) and (c) show a plot of feed-motor current signals with the two distinct changes: from entry

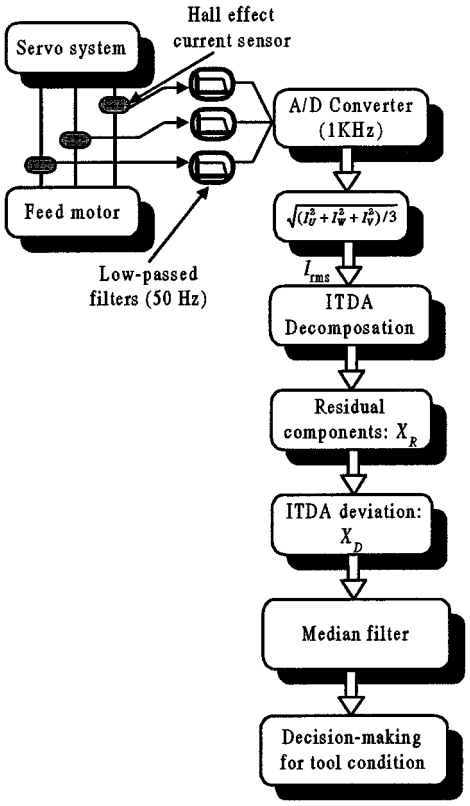

Fig. 7. Experimental set-up.

cut to steady-state cut and from steady-state cut to exit cut, respectively. Whilst can be seen from the steady-state phase of the feed-motor current signal, a high degree of runout is presented in the end milling processing as well as a high level of noise. Fig. 8(b) and (d) shows a plot of the processed feed-motor current signals corresponding to the float thresholds in Fig. 8(a) and (c), respectively. As can be seen from the figures, all of the processed feed-motor current signals are well under the detection limits, thus demonstrating the *robustness* of the algorithm to entry, exit, runout, and noise sources in the feed-motor current signal.

B. Flute Breakage During Steady-State Cutting

In this case, the flute breakage occurred during the steady-state cutting. The feed-motor current signals for this case are shown in Fig. 9(a), the breakage event occurred in the row current signal at the 1.15 s, one flute of cutting tools is broken for the event. The unusually high degree of runout occurred in this system, as only three of the four flutes were performing essentially all of the cuttings. Fig. 9(b) shows the results obtained by the flute breakage detection algorithm, the processed feed-motor current exceeds the float threshold at the 1.25 s. The delay time for 0.10 s is resulted by the detection algorithm. The algorithm can detect the flute breakage successfully. In terms of the practical test, the monitoring system needs to take a 0.275 s to identify the tool flute breakage, the time refers to the collections of current signals to the alarms, including the calculation time of algorithm, and the delay time resulted by the algorithm. Note that the computer used is *PII, CUP* 433 MHz. Clearly, the times can meet the need of the practical application for monitoring tool flute breakage during end milling.

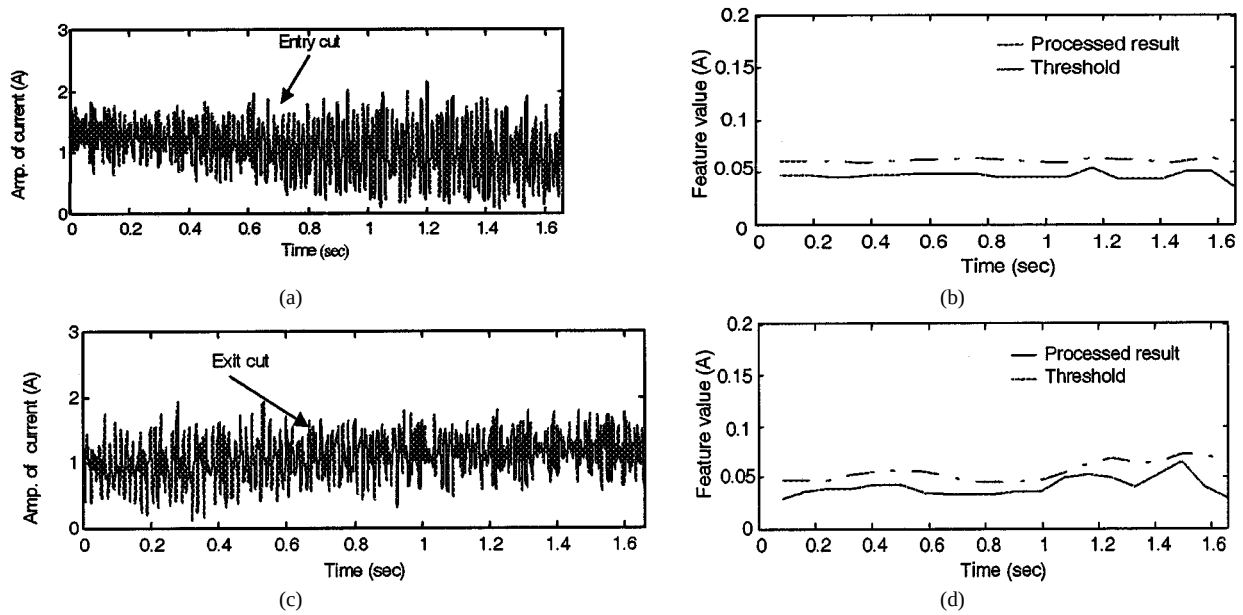

Fig. 8. Entry/exit cut test in end milling. Tool/workpiece material: HSS/45# steel; spindle speed: 900 rpm; radial depth of cut: 2 mm; axial depth of cut: 4 mm; feed speed: 120 mm/min; cutter diameter: 8 mm; cutter flute: 4. (a) Feed-motor current signal with entry cut. (b) Processed result of entry cut. (c) Feed-motor current signal with exit cut. (d) Processed result of exit cut.

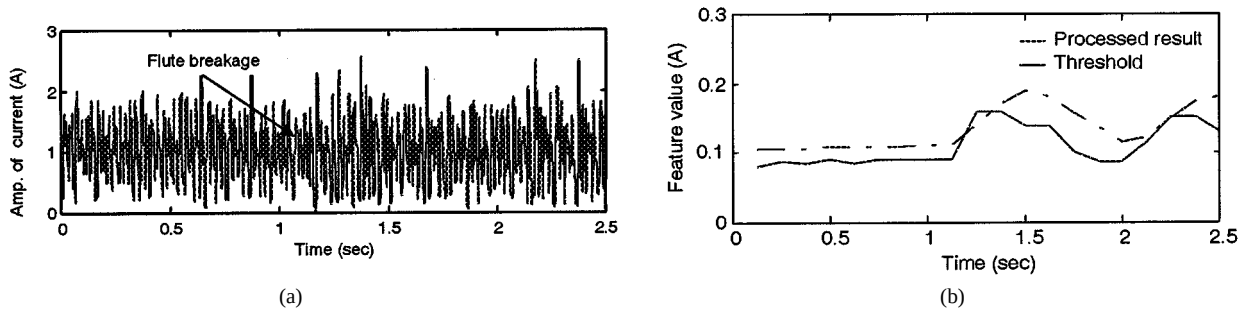

Fig. 9. Flute breakage during the steady-state end milling. Tool/workpiece material: HSS/45# steel; spindle speed: 600 rpm; radial depth of cut: 4 mm; axial depth of cut: 4 mm; feed speed: 120 mm/min; cutter diameter: 8 mm; cutter flute: 4. (a) Feed-motor current signal with flute breakage. (b) Processed result of one flute breakage.

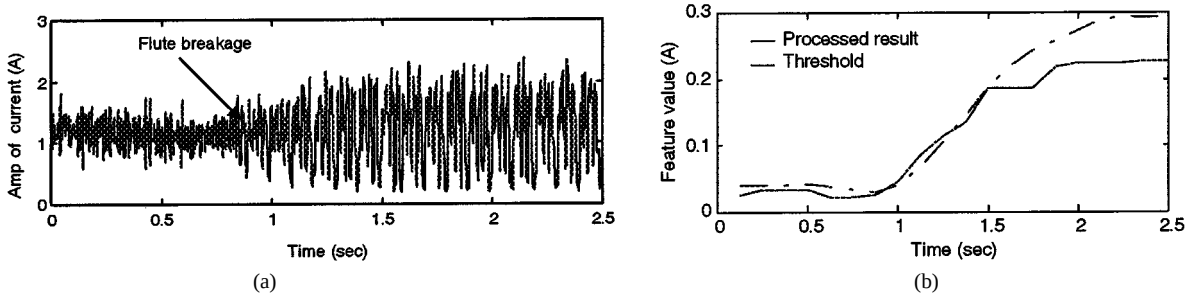

Fig. 10. Flute breakage on entry cut. Tool/workpiece material: HSS/45# steel; spindle speed: 600 rpm; radial depth of cut: 4 mm; axial depth of cut: 4 mm; feed speed: 90 mm/min; cutter diameter: 6 mm; cutter flute: 4. (a) Feed-motor current signal with flute breakage on entry cut. (b) the processed results of one flute breakage.

C. Flute Breakage on Entry/Exit Cut

The tests come on conforming the ability of the detection algorithm to quickly and reliably detect flute breakage during end milling. The flute breakage of some cutters in end milling usually occurs on entry/exit cut. Fig. 10(a) is a plot of the feed-motor current signals when cutter entries in the workpiece, as well as the cutter, occurs one flute breakage. The result of detection algorithm is shown in Fig. 10(b). Fig. 11(a) is plot of the cutter broken upon exit from the workpeice, two flutes of the cutting tools are broken for the event, the processed results of the feed-motor current signals is shown in Fig. 11(b). For the two cases, the flute breakage can be successfully detected by the detection algorithm through the comparison between the processed current signals and the float threshold.

D. Effect of Cutting Parameters

An effective algorithm for detecting flute breakage in end milling also should be insensitive to the changes of the cut-

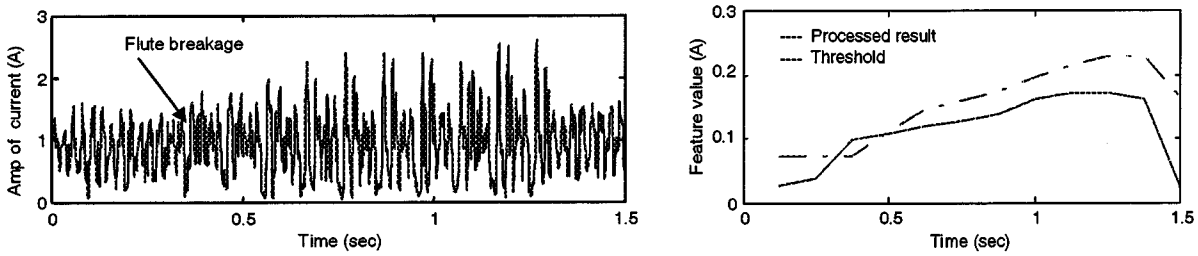

(a) (b)

Fig. 11. Flute breakage on exit cut. Tool/workpiece material: HSS/45# steel; spindle speed: 600 rpm; radial depth of cut: 2 mm; axial depth of cut: 4 mm; feed speed: 120 mm/min; cutter diameter: 6 mm; cutter flute: 4. (a) Feed-motor current signal with flute breakage on exit cut. (b) The processed results of two flutes breakage.

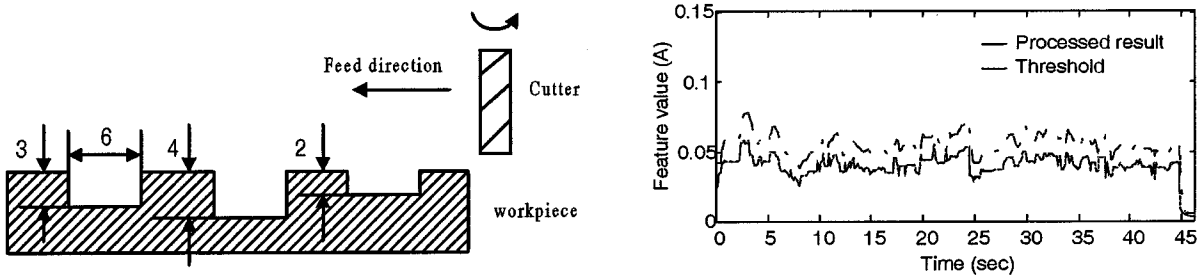

(a) (b)

Fig. 12. Feed-motor current signals when cutting workpiece with grooves. Tool/workpiece material: HSS/45# steel; spindle speed: 900 rpm; radial depth of cut: 4 mm; axial depth of cut: 4 mm; feed speed: 120 mm/min; cutter diameter: 6 mm; cutter flute: 4. (a) Workpiece. (b) The processed results of the feed-motor current.

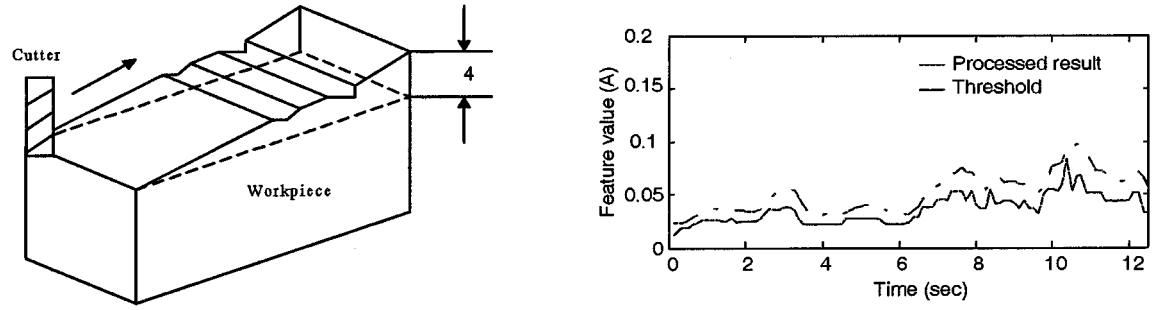

(a) (b)

Fig. 13. Feed-motor current signals when cutting irregular workpiece. Tool/workpiece material: HSS/45# steel; spindle speed: 900 rpm; radial depth of cut: 4 mm; axial depth of cut: 0–4 mm; feed speed of cut: 120 mm/min; cutter diameter: 6 mm; cutter flute: 4. (a) Workpiece. (b) The processed results of the feed-motor current.

ting parameters. Radial depth of cut and axial depth of cut in end milling is affected by the workpiece shape, like step, groove, and slope, and so on. The final tests are to verify the insensitivity of the algorithm of flute breakage detection to the changes of cutting parameters for end milling. The typical workpieces, which results in changes of radial or axial depth of cut, are shown in Figs. 12(a) and 13(a). Some grooves with different depth were on the surface of workpiece in Fig. 12(a), these grooves result in the change of axial depth of cut during end milling, thus the feed-motor current signals are not steady. The processed result of the feed-motor current, however, is insensitive to these changes during end milling in Fig. 12(b). Fig. 13(a) also is a typical workpieces, which are effective to the changes of cutting parameters, such as the axial depth of cut. The feed-motor current signals in the case are not steady, yet. The processed result of the above feed-motor current is shown in Fig. 13(b) correspondingly. From the results of Figs. 12(b) and 13(b), the monitoring feature of the feed-motor current is insensitive to the change of cutting parameters during end milling.

According to these test results, the algorithm presented for detecting flute breakage detection could have high robustness and effective ability to be applied to feed-motor current signals in real time for practical end milling.

VI. Conclusions

In this paper, an algorithm for detecting flute breakage during end milling, based on improved time-domain averaging, has been proposed using the feed-motor current signals. Firstly, the improved time-domain averaging for analyzing repetitive signals has been addressed and analyzed, and applied to analyze feed-motor current signal derived from end milling. Secondly, an effective algorithm for detecting flute breakage has been proposed, including the selection of monitoring feature and the establishing of float threshold. The detection approach has been

demonstrated to be effective in different cases through a set of experiments. Conclusion that may be made as a result of the paper include:

1) The traditional algorithm of such direct TDA hides a question of the period cutting error that has a large bad influence on the decomposed results. In terms of the analysis results of experiments, if the number of averaging period is selected as a large value, the influence of period cutting error will lead that the decomposed results are not at all useful.
2) The improved time-domain averaging (ITDA) can effectively avoid the influence of the period cutting error, the number of averaging period can be randomly selected associated with the requirements of experiments.
3) The detection strategy requires no trial cuts to establish a float threshold limit as the algorithm detection criteria is based on the variability of cutting parameters.
4) The monitoring system based on the improved TDA and the float threshold can rapidly detect the flute breakage during end milling, only needing about 0.3 s before the alarm indicates tool flute breakage.
5) The detection system is robust to the effects of cutting conditions full of variety, including the effects of entry/exit cut, change of cutting parameters, and runout in the feed-motor current signals. Particularly, the tool flute breakage during entry/exit cut could be detected successfully, and the algorithm is insensitive to the runout, entry/exit cut, and change of axial or radial depth of cut during end milling.
6) Furthermore, the advantages of the monitoring system by comparison with the others is a simple and inexpensive sensor, does not interrupt the cutting process, effective algorithm, high robustness, and application to practical end milling in real time. Unlike the other works, the motor current is only used to estimate cutting force using a model, and then the estimated cutting force is used to detect tool conditions. In this paper, the feed-motor is directly applied to detect the tool flute breakage. Therefore, the monitoring system based on the approach above is a very simple and low-cost.

Additionally, although all experiments were limited to end milling operations, it is believed that the detection approach may be applied equally well to other milling operations.

ACKNOWLEDGMENT

The author gratefully acknowledges the reviewers' suggestions for improving the paper. The author also thanks S. W. Cheng at the Department of Manufacturing Engineering, City University of Hong Kong for kind help during the experiments and the Alexander von Humboldt Foundation for revisions made to the paper.

REFERENCES

[1] Y. Altintas and I. Yellowley, "In process detection of tool failure in milling using cutting force models," *ASME Trans. J. Eng. Ind.*, vol. 111, pp. 149–159, 1989.
[2] J. H. Tarn and M. Tomizuka, "On-line monitoring of tool and cutting conditions in milling," *ASME Trans. J. Eng. Ind.*, vol. 111, pp. 206–212, 1989.
[3] Y. Altintas, "In-process detection of tool breakage's using time series monitoring of cutting forces," *Int. J. Mach. Tools Manuf.*, vol. 28, no. 2, pp. 157–172, 1988.
[4] D. J. O'Brien, J. W. Sutherland, and S. G. Kapoor, "A force-based approach to on-line flute breakage detection in a peripheral end milling process," *ASME, Dynamic Syst. Contr. Div. DSC*, vol. 22, pp. 25–30, 1990.
[5] M. S. Lan and D. A. Dornfeld, "In-process tool fracture detection," *ASME Trans. J. Eng. Materials Technol.*, vol. 106, no. 2, p. 111, Apr. 1984.
[6] S. A. Inasaki and S. Fuduoka, "Monitoring system for cutting tool failure using an acoustic emission sensor," *Int. J. JSME*, vol. 30, pp. 323–328, 1987.
[7] E. Emel and E. Jr. Kannatey-Asibu, "Tool failure monitoring in turning by pattern recognition analysis of AE signals," *ASME Trans. J. Eng. Ind.*, vol. 110, no. 2, pp. 137–145, May 1988.
[8] S. V. Kamarti, S. R. T. Kumara, and P. H. Cohen, "Flank wear estimation in turning through wavelet representation of acoustic emission signals," *ASME Trans. J. Manuf. Sci. Eng.*, vol. 122, pp. 12–19, 2000.
[9] D. V. Hutten and F. Hu, "Acoustic emission monitoring of tool wear in end milling using time-domain averaging," *ASME Trans. J. Manuf. Sci. Eng.*, vol. 121, pp. 8–12, 1999.
[10] X. Li and Z. Yuan, "Tool wear monitoring with wavelet packet transform-fuzzy clustering method," *Wear*, vol. 219, pp. 145–154, 1998.
[11] K. Matsushima, K. Bertok, and T. Sata, "In process detection of tool breakage by monitoring the spindle current of a machine tool," *ASME J. Meas. Contr. Batch Manuf.*, pp. 145–154, 1982.
[12] Y. Altintas, "Prediction of cutting forces and tool breakage in milling from feed drive current measurements," *ASME Trans. J. Eng. Ind.*, vol. 114, pp. 386–392, 1992.
[13] J. M. Lee, D. K. Choi, and C. N. Chu, "Real time tool breakage monitoring for NC milling process," *Annals CIRP*, vol. 44, no. 1, pp. 59–62, 1995.
[14] S. Braun and B. Seth, "Analysis of repetitive mechanism signatures," *J. Sound Vib.*, vol. 70, no. 4, pp. 513–526, 1980.
[15] P. W. Prickett and C. Johns, "An overview of approach to end milling tool monitoring," *Int. J. Mach. Tools Manuf.*, vol. 39, no. 2, pp. 105–122, 1999.
[16] J. C. Chen and J. T. Black, "A fuzzy-nets in process system for tool breakage monitoring in end milling operations," *Int. J. Mach. Tools Manuf.*, vol. 37, no. 6, pp. 783–800, 1997.
[17] Y. S. Tarng and B. Y. Lee, "Use of model-based cutting simulation systems for tool breakage monitoring in milling," *Int. J. Mach. Tools Manuf.*, vol. 32, no. 5, pp. 641–649, 1992.
[18] G. I. Kim, T. W. Kwon, and N. C. Chong, "Indirect cutting force measurement and cutting force regulation using spindle motor current," *Int. J. Manuf. Sci. Technol.*, vol. 1, no. 1, pp. 46–54, 1999.
[19] H. Lu, H. Zou, C. Jiang, and L. Qu, "An improved algorithm for direct time domain averaging," *Mech. Syst. Signal Processing*, vol. 14, no. 2, pp. 279–285, 2000.
[20] X. Li, D. Alexandar, and K. V. Patri, "Current sensor-based feed cutting force intelligent estimation and tool wear condition monitoring," *IEEE Trans. Ind. Electron.*, vol. 47, pp. 697–702, June 2000.
[21] I. Tansel, M. Trujillo, A. Nedbouyan, C. Velez, W. Bao, T. T. Arkan, and B. Tansel, "Micro-end-milling—III. Wear estimation and tool breakage detection using acoustic emission signals," *Int. J. Mach. Tools Manuf.*, vol. 38, no. 12, pp. 1449–1466, 1998.
[22] B. Lee, H. Liu, and Y. Tarng, "Monitoring of tool fracture in end milling using induction motor current," *J. Mater. Processing Technol.*, vol. 70, no. 1–3, pp. 279–284, 1997.

Xiaoli Li received the B.S.E. and M.S.E. degrees from Kun-ming University of Science and Technology, Kun-ming, China, and the Ph.D. degree from Harbin Institute of Technology, Harbin, China, in 1992, 1995, and 1997, respectively, all in mechanical engineering.

From 1998 to 2000, he was a Research Fellow of the Department of Manufacturing Engineering, City University of Hong Kong, Hong Kong. He is currently a Research Fellow of the Alexander von Humboldt Foundation, and works in the Institute for Production, Engineering and Machine Tools, Hannover University, Hannover, Germany. His research interests include manufacturing process monitoring, machining error compensation, intelligent technology, applied signal processing, and bio-signal processing. He has published 28 international journal papers, and two books.